

Optimized Wind Turbine Emulator based on an AC to DC Motor Generator Set

Yahya Aljarhizi

Laboratory of Materials and Subatomic Physics, Faculty of Sciences, Ibn Tofail University, Morocco
aljarhizi.yahya@gmail.com
(corresponding author)

Ayoub Nouaiti

Laboratory of Computer Science, Applied Math and Electrical Engineering Department, Moulay Ismail University, IEVIA Team, Morocco
nouayoub@gmail.com

Elmehdi Al Ibrahim

Laboratory of Materials and Subatomic Physics, Faculty of Sciences, Ibn Tofail University, Morocco
alibrahmielmehdi@yahoo.fr

Chaymaa Boutahiri

Laboratory of Computer Science, Applied Math and Electrical Engineering Department, Moulay Ismail University, IEVIA Team, Morocco
chaymaaboutahiri@gmail.com

Abdelilah Hassoune

Laboratory of Energy & Electrical Systems, Ecole Nationale Supérieure d'Electricite et de Mecanique, Morocco | Hassan II University of Casablanca, Morocco
a.hassoune@IEEE.org

Abdelouahed Mesbahi

Laboratory of Energy & Electrical Systems, Ecole Nationale Supérieure d'Electricite et de Mecanique, Morocco | Hassan II University of Casablanca, Morocco
abdelouahed.mesbahi@gmail.com

Received: 12 February 2023 | Revised: 4 March 2023 | Accepted: 8 March 2023

ABSTRACT

This study presents an Optimized Wind Turbine Emulator (OWTE) based on a DC generator driven by a three-phase Induction Motor (IM). The IM speed is varied using an AC drive that converts fixed RMS voltage and frequency to variable ones due to v/f control. The frequency reference of the control was calculated through optimized equations of a wind turbine model for maximum power and torque. The overall system was simulated on Matlab/Simulink using a wind speed profile scenario. An experimental test bench controlled by a TMS320F28379D card was set up in the laboratory to confirm the effectiveness of the obtained simulation results.

Keywords-wind power conversion system; Wind Turbine Emulator (WTE); induction motor; DC generator; Variable Frequency Drive (VFD)

I. INTRODUCTION

The growing interest in using wind energy has led many researchers to experiment with emulators instead of real power

systems, due to the high investment cost of setting up a wind turbine and the slow dynamics of wind speed. Emulators are used to reproduce the characteristics developed by wind turbines for given wind speed profiles [1-2], and several

different emulators have been suggested. Some are based on permanent magnet synchronous machines [3], DC, or induction motors to replace the mechanical part [4-6]. Many electrical machines have been considered for the generator part, such as self-excited induction generators [7-8], permanent magnet synchronous generators [9-10], or DC generators [11]. The study of emulators focuses on several parameters such as the generator speed, pitch angle, maximum power, and torque [12]. Digital circuits, including FPGAs, microcontrollers, and DSP cards are used to apply efficient control algorithms with these emulators [13-14].

This work was based on an electromechanical system designed to achieve an efficient model of the conversion system as an Optimized Wind Turbine Emulator (OWTE). The OWTE was made up of a DC generator driven by an induction motor monitored through a v/f control. The speed reference was generated from the derived equations of power and torque in the maximum states. The model was simulated in MATLAB/Simulink and analyzed to test its effectiveness. In addition, an experimental setup was set up in the laboratory, where the adopted control was implemented on a Texas Instruments digital signal processing cardboard to provide more credibility and experimental verification of the results.

II. DESCRIPTION AND MODELING OF THE PROPOSED SYSTEM

Figure 1 shows the structure of the proposed system, which is composed of an Optimized Wind Turbine Model (OWTM), a Variable Frequency AC Drive (VFD), and an AC to DC Motor Generator Set (M-G).

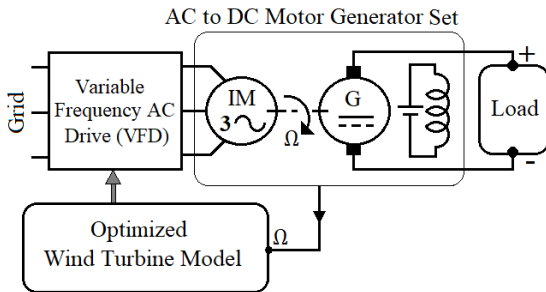


Fig. 1. The proposed system of the OWTE.

A. Wind turbine Model

A Wind Turbine (WT) transforms the kinetic energy taken by the blades into mechanical torque at the rotor shaft. However, the geometry of the turbine, the wind speed (V_w), and the pitch angle (β) of the blades have an essential influence on its performance [15]. The aerodynamic power depends on the wind power and the power coefficient C_p :

$$P_w = \frac{1}{2} A \rho V_w^3 C_p(\lambda, \beta) \quad (1)$$

where ρ is the air density, and A is the area swept by the rotor blades given by πR^2 and R is the turbine radius. $C_p(\lambda, \beta)$ is the ratio between P_w and V_w , which depends on β and λ being the pitch angle and the Tip-Speed-Ratio (TSR), respectively. λ can be obtained from:

$$\lambda = \frac{\Omega R}{V_w} \quad (2)$$

where Ω is the angular velocity.

Moreover, many studies have been conducted to define the appropriate expression of C_p , while others proposed functions that can approximately represent the real curve of the power coefficient. Polynomial, sinusoidal, and exponential function models are usually used to model the power coefficient [16]. The sinusoidal and exponential function models are related to λ and β to control the required C_p . The polynomial function model assumes that the attack angle of the wind turbine blade is constant. This model makes C_p a simple function that depends on a specific λ [17]. The adopted model is based on the exponential function expressed by:

$$C_p(\lambda, \beta) = c_1 \left(c_2 \frac{1}{\lambda^i} - c_3 \beta - c_4 \beta^{c_5} - c_6 \right) e^{-c_7 \frac{1}{\lambda^i} + c_8 \lambda} \quad (3)$$

with:

$$\frac{1}{\lambda^i} = \frac{1}{\lambda + a_9 \beta} - \frac{a_{10}}{\beta^3 + 1} \quad (4)$$

Some studies adjusted the exponential function model to obtain a specified C_p curve by choosing the coefficient values c_i [18]. An ideal wind turbine can obtain only 59.25% mechanical energy from the overall kinetic wind energy, known as the Betz limit [19]. However, the aerodynamic torque of the wind turbine T_w is a relation between the mechanical power and the angular velocity:

$$T_w = \frac{1}{2} \frac{\pi \rho R^2 V_w^3 C_p(\lambda, \beta)}{\Omega} \quad (5)$$

Figure 2 shows the mechanical model of the WT conversion system. Turbine blades and the electromechanical converter are among the main components of the WT system, as well as the gearbox with its gain G , which is a mediator between the low-rotation shaft Ω_t and the high-rotation shaft Ω_m [20-21].

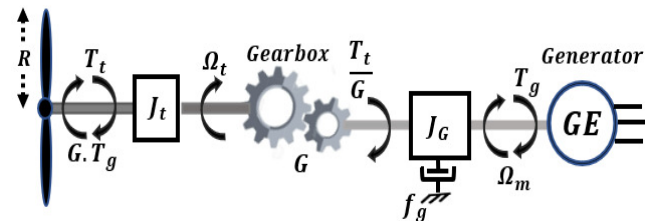


Fig. 2. Mechanical model of the WT conversion system.

Equation (6) describes the basic mechanical equation Ω_m for the high-speed shaft tied to an electrical generator, whereas (7) expresses the equivalent inertia J acted on the high-speed shaft, i.e., the generator side [21]:

$$\frac{T_t}{G} - T_g = J \frac{d\Omega_m}{dt} \quad (6)$$

$$J = \frac{J_t}{G^2} + J_g \quad (7)$$

where T_t and T_g are the corresponding turbine and generator torques and J_t and J_g are the low-speed (turbine side) and high-speed (generator side) inertia shafts, respectively. Figure 3

shows the static and dynamic characteristics based on the above equations to provide a realistic WT model [21-22]. The adopted model was verified in Matlab/Simulink based on the parameters in Table I. Figure 4 shows the obtained curve of C_p based on (3), where the chosen c_i values are listed in Table II.

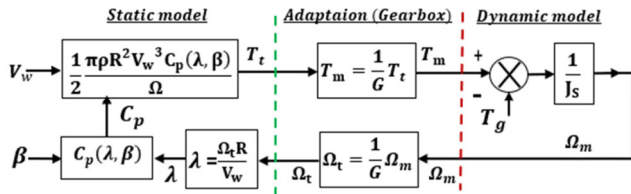


Fig. 3. Overall wind turbine model.

TABLE I. PARAMETERS OF THE WIND TURBINE MODEL

Parameters	Values
Rated power	10KW
Cut-in wind speed	3.0m/s
Rated wind speed	10m/s
Rotor diameter	7.1m
Gear	7
Number of blades	3

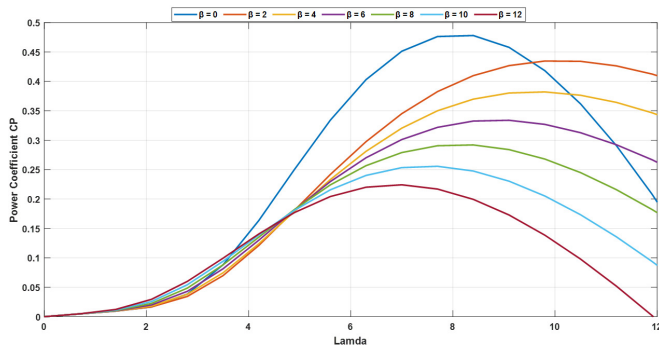


Fig. 4. Curve of the power coefficient C_p .

TABLE II. PARAMETERS OF THE POWER COEFFICIENT

c_1	c_2	c_3	c_4	c_5
0.5175	116	0.4	0	0
c_6	c_7	c_9	a_9	a_{10}
5	21	0.0068	0.08	0.035

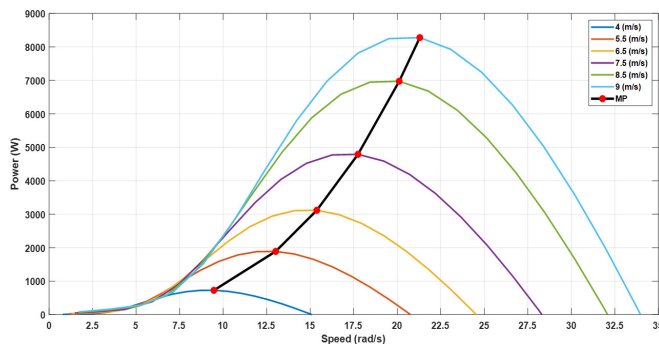


Fig. 5. Wind turbine power versus angular speed.

As shown in Figure 4, several curves were deployed based on various pitch angles. However, only the curve corresponding

to $\beta=0^\circ$ will be considered in this paper with $\lambda=8.1$ that will be defined as the optimal λ_{opt} , as a result of the achieved maximum value of the power coefficient $C_{pmax}=0.48$ [23]. Figures 5 and 6 show the mechanical power and torque characteristics of the wind turbine model used versus the angular speed. The Maximum Power (MP) and Torque (MT) curves shown in Figures 5 and 6 are the main structure of the OWTM.

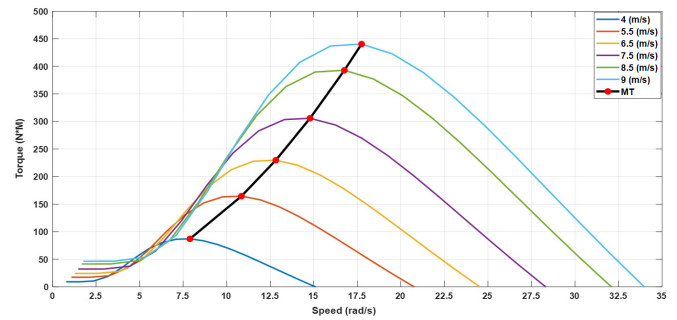


Fig. 6. Wind turbine torque versus angular speed.

B. Variable Frequency AC Drive

Figure 7 shows the major components of a PWM-based VFD: non-controlled three-phase rectifier, DC bus/filter, and the three-phase inverter with its control unit.

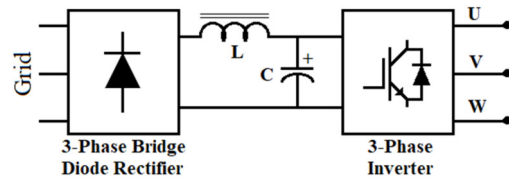


Fig. 7. Structure of a PWM-based VFD.

The VFD varies the speed of the induction motor based on v/f control to keep the torque constant [24]. Figure 8 presents the variation of the stator voltage of IM versus frequency. The linear zone in the range $[f_{min} - f_{rated}]$ will be used to generate an adequate v/f profile for the control unit.

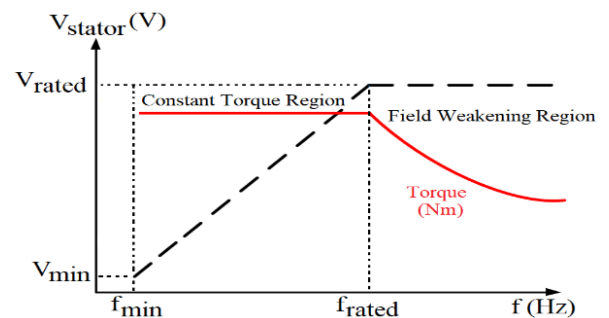


Fig. 8. Variation of IM voltage versus frequency.

C. AC to DC Motor Generator Set

The M-G set used consists of a three-phase induction motor (squirrel-cage) coupled directly to a DC generator (DC-G). The

IM will produce a variable speed to the DC-G. This latter will produce a variable power according to the wind speed profile.

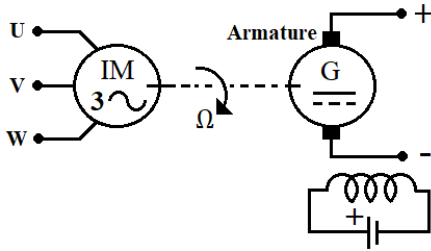


Fig. 9. The M-G set association.

III. THE ADOPTED CONTROL METHOD

Figure 10 shows the adopted OWTM with the VFD and the M-G set, which operates at the optimal $C_{pmax}=0.48$ and $\lambda_{opt}=8.1$.

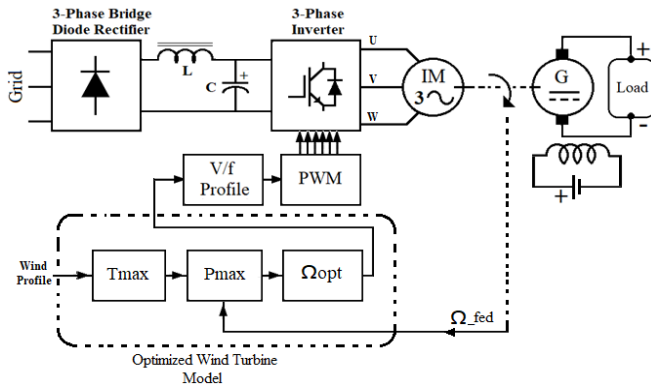


Fig. 10. Block diagram of the proposed OWTM.

The maximum torque and power expressions obtained from Figures 5 and 6, using the curve fitting tool in Matlab, are:

$$T_{max} = 5.437 V_W^2 - 1.506 * 10^{-13} \tag{8}$$

$$P_{max} = 0.857 \Omega_{opt}^3 + 3.505 * 10^{-13} \tag{9}$$

The sensed angular speed Ω_{fed} of the IM and the wind profile speed were employed to obtain the maximum power using (8). Then, the reference angular speed Ω_{opt} was obtained according to (9). After that, the frequency reference f_{ref} of the VFD was generated for the three-phase inverter. The v/f profile was determined for a rated frequency and voltage of 50Hz and 380V. Three sinusoidal reference signals were generated and compared with a carrier triangular signal to control the inverter switches.

IV. SIMULATION RESULTS

The proposed system was modeled in Matlab/Simulink, as shown in Figure 11, using an M-G set of 1.5KW and a load of 122Ω. This simulation aimed to analyze the response of the optimized wind turbine emulator when it is exposed to a variable wind profile scenario between 4-9m/s. Figures 12-15 show the results obtained for 12s.

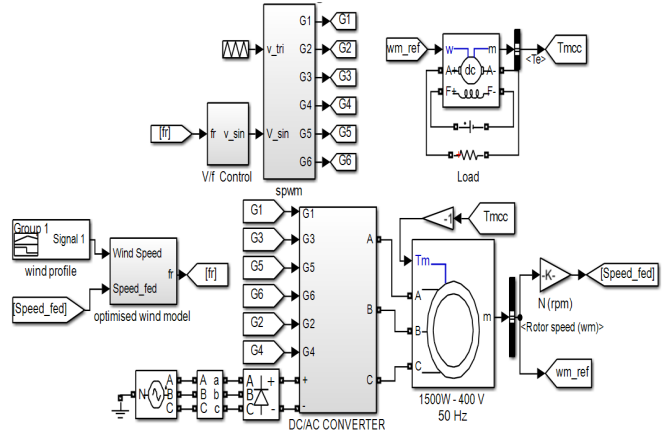


Fig. 11. Simulink model diagram of the proposed OWTM.

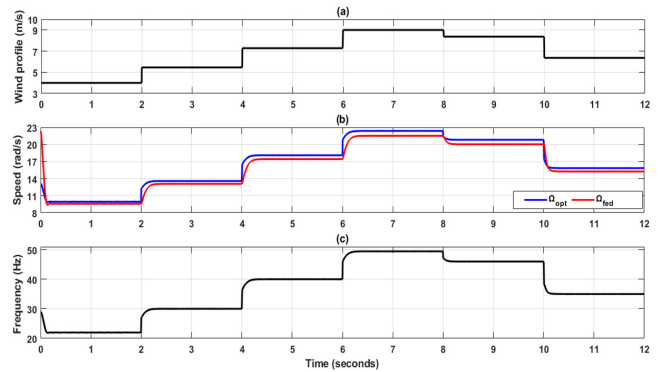


Fig. 12. Simulation results: (a) V_w (m/s), (b) Ω_{opt} and Ω_{fed} (rad/s), (c) f_{ref} (Hz).

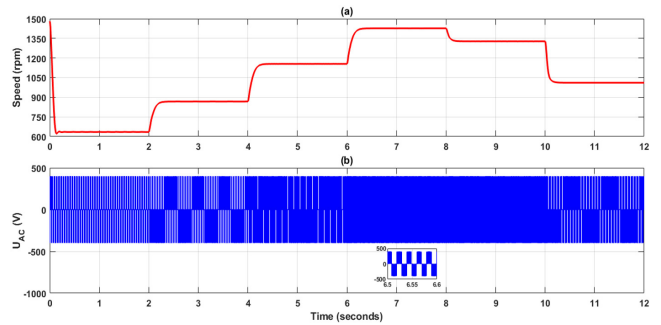


Fig. 13. Simulation results: (a) N_{IM} (rpm), (b) U_{AC} (V).

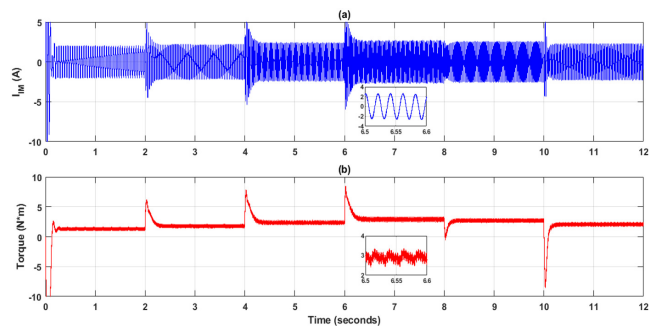


Fig. 14. Simulation results: (a) I_{IM} (A), (b) Torque (Nm).

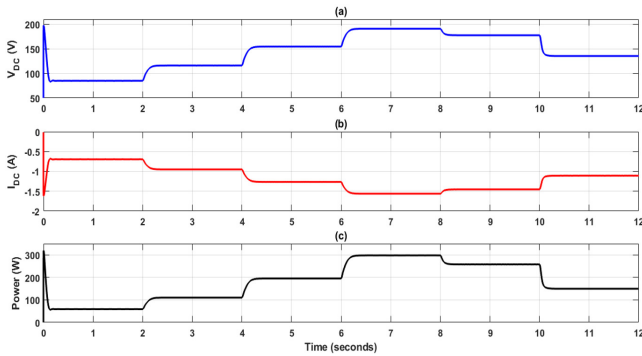


Fig. 15. Simulation results (a) V_{DC} (V); (b) I_{DC} (A); (c) Power (W).

As shown in Figure 12, the optimal speed Ω_{opt} follows the wind speed scenario. The difference between Ω_{opt} and the speed produced by the induction motor Ω_{fed} is justified by the slip. The calculated f_{ref} , which varied between 20-50Hz, was used to control the VFD. The output AC voltage of the VFD has three levels with a variable frequency and RMS value, as shown in Figure 13. The rotational speed N_{IM} varied between 600-1430rpm. However, the obtained torque, shown in Figure 14, was almost constant due to the v/f control. The same remark was noted for the IM current, which was also sinusoidal in shape. According to Figure 15, the generated power of the DC-G pursued the different variations of wind speed, which provided the main outcomes of the OWTE. The DC voltage varied in the 85-200V interval. The DC current changed from -1.6 to -0.6A, the negative values were due to the generator operating mode in Simulink, whereas the power variation was between 55-300W. These results show that the system effectively reproduced the static and dynamic characteristics of the wind turbine for the maximum value under different wind conditions.

V. EXPERIMENTAL RESULTS

Figure 16 shows the proposed hardware rig of the OWTE, consisting of a variable speed drive, namely Altivar 18, and a 1.5KW three-phase induction motor coupled to a DC machine that fed a resistive load of 122Ω. A TMS320F28379D launchpad card was used to control the VFD. Current and velocity hall-effect sensor cards were used to sense voltage. Data acquisition in real-time was carried out in Matlab using a NI 6009 card.

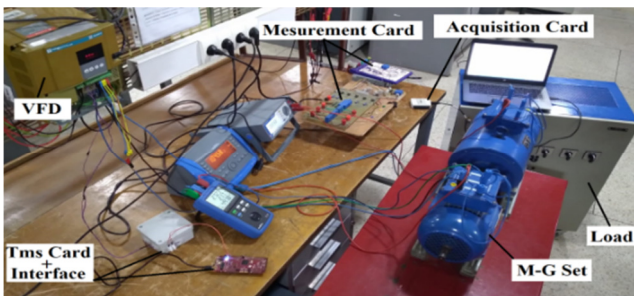


Fig. 16. Test bench of the proposed system.

The proposed system was verified experimentally using the same wind profile scenario as the simulation. Figures 17 and 18

illustrate the main results for 60s. The rotational speed N_{IM} , shown in Figure 17, varies with the wind profile between 500-1430rpm. In the same figure, the AC voltage with three levels has a variable frequency and RMS value, and the IM current is sinusoidal in form. Figure 18 shows the variation of the generated DC power across the load between 10-320W. The DC voltage was established in the 10-210V interval and the DC current was between 0.4-1.7A. The experimental results confirmed the simulations and validated the proposed emulator.

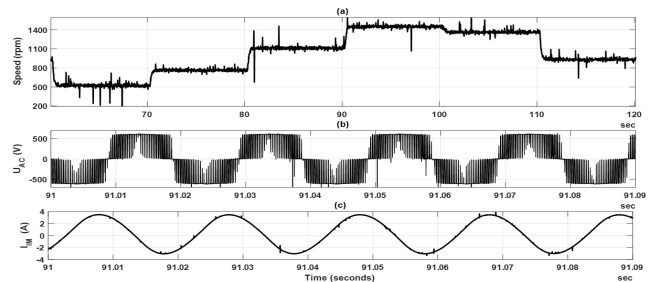


Fig. 17. Experimental results: (a) N_{IM} (rpm), (b) U_{AC} , (c) I_{IM} .

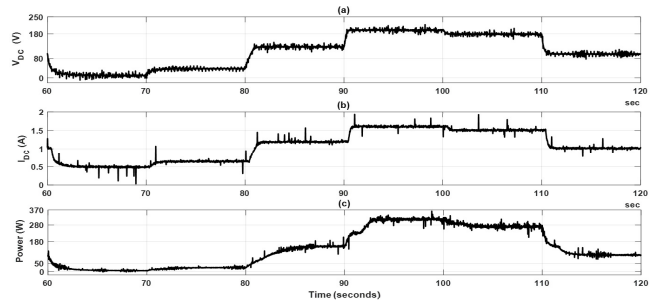


Fig. 18. Experimental results: (a) V_{DC} , (b) I_{DC} , (c) Power.

VI. CONCLUSION

This paper presented an efficient structure of a wind turbine emulator based on an optimized model. This emulator system consists of an induction motor connected directly to a DC generator to reproduce the same dynamic behavior of a wind turbine, such as the torque, mechanical power, and angular speed. Considering the turbine model with a fixed pitch angle, the used control extracts the maximum power using simple fitting equations of power and torque curves. Based on the simulation and experimental results, the proposed WTE can effectively emulate the behavior of a real wind turbine, and the control method achieved good tracking of wind speed variation. In future work, the proposed OWTE will be developed by testing other structures and controls with the possibility of injecting energy into the grid.

REFERENCES

[1] S. Benzaouia, M. Mokhtari, S. Zouggar, A. Rabhi, M. L. Elhafyani, and T. Ouchbel, "Design and implementation details of a low cost sensorless emulator for variable speed wind turbines," *Sustainable Energy, Grids and Networks*, vol. 26, Jun. 2021, Art. no. 100431, <https://doi.org/10.1016/j.segan.2021.100431>.

[2] T. Ahmed, M. H. Baloch, N. Khan, G. Mehr, B. A. Mirjat, and Y. A. Memon, "Experimental Analysis and Control of a Wind-Generator System through a DC-DC Boost Converter for Extremum Seeking,"

- Engineering, Technology & Applied Science Research, vol. 11, no. 1, pp. 6714–6718, Feb. 2021, <https://doi.org/10.48084/etasr.3948>.
- [3] M. E. Abdallah, O. M. Arafa, A. Shaltot, and G. A. A. Aziz, "Wind turbine emulation using permanent magnet synchronous motor," *Journal of Electrical Systems and Information Technology*, vol. 5, no. 2, pp. 121–134, Sep. 2018, <https://doi.org/10.1016/j.jesit.2018.03.005>.
- [4] T. F. dos Santos *et al.*, "Wind Turbine Emulator with DC Motor," in *2019 IEEE 15th Brazilian Power Electronics Conference and 5th IEEE Southern Power Electronics Conference (COBEP/SPEC)*, Santos, Brazil, Sep. 2019, pp. 1–6, <https://doi.org/10.1109/COBEP/SPEC44138.2019.9065694>.
- [5] I. Moussa and A. Khedher, "Soft-switching inverter investigation for three-phase IM drive as wind turbine emulator design," *Microelectronics Reliability*, vol. 138, Nov. 2022, Art. no. 114722, <https://doi.org/10.1016/j.microrel.2022.114722>.
- [6] L. Benaouinate, M. Khafallah, A. Mesbahi, and A. Martinez, "Development of a useful wind turbine emulator based on permanent magnet DC motor," in *2017 14th International Multi-Conference on Systems, Signals & Devices (SSD)*, Marrakech, Morocco, Mar. 2017, pp. 44–48, <https://doi.org/10.1109/SSD.2017.8166972>.
- [7] Y. Aljarhizi, E. M. A. Ibrahim, A. Mesbahi, A. Hassoune, and M. Khafallah, "Static Power Converters for a Wind Turbine Emulator Driving a Self-Excited Induction Generator," in *2020 1st International Conference on Innovative Research in Applied Science, Engineering and Technology (IRASET)*, Meknes, Morocco, Apr. 2020, pp. 1–6, <https://doi.org/10.1109/IRASET48871.2020.9092319>.
- [8] G. Mustafa, M. H. Baloch, S. H. Qazi, S. Tahir, N. Khan, and B. A. Mirjat, "Experimental Investigation and Control of a Hybrid (PV-Wind) Energy Power System," *Engineering, Technology & Applied Science Research*, vol. 11, no. 1, pp. 6781–6786, Feb. 2021, <https://doi.org/10.48084/etasr.3964>.
- [9] T. Boutabba, S. Drid, F. Mechnan, and L. Chrifi-Alaoui, "Design of Small Wind Turbine Emulator Based on dSPACE 1104," Jan. 2023, <https://doi.org/10.21203/rs.3.rs-2429680/v1>.
- [10] A. Mesbahi, Y. Aljarhizi, A. Hassoune, M. Khafallah, and E. Alibrahmi, "Boost Converter implementation for Wind Generation System based on a variable speed PMSG," in *2020 1st International Conference on Innovative Research in Applied Science, Engineering and Technology (IRASET)*, Meknes, Morocco, Apr. 2020, pp. 1–6, <https://doi.org/10.1109/IRASET48871.2020.9092143>.
- [11] G. Gökkuş and A. Kulaksız, "Design and implementation of a wind turbine emulator using an induction motor and direct current machine," *International Journal of Renewable Energy Research*, vol. 10, no. 3, pp. 1426–1498, Sep. 2020.
- [12] I. Yahyaoui and A. S. Cantero, "Modeling and Characterization of a Wind Turbine Emulator," in *Advances in Renewable Energies and Power Technologies*, I. Yahyaoui, Ed. Amsterdam, Netherlands: Elsevier, 2018, pp. 491–508.
- [13] P. Satish Kumar, R. P. S. Chandrasena, and K. Victor Sam Moses Babu, "Design and implementation of wind turbine emulator using FPGA for stand-alone applications," *International Journal of Ambient Energy*, vol. 43, no. 1, pp. 2397–2409, Dec. 2022, <https://doi.org/10.1080/01430750.2020.1736152>.
- [14] K. Premkumar *et al.*, "Black Widow Optimization-Based Optimal PI-Controlled Wind Turbine Emulator," *Sustainability*, vol. 12, no. 24, Jan. 2020, Art. no. 10357, <https://doi.org/10.3390/su122410357>.
- [15] J. Wen, L. Zhou, and H. Zhang, "Mode interpretation of blade number effects on wake dynamics of small-scale horizontal axis wind turbine," *Energy*, vol. 263, Jan. 2023, Art. no. 125692, <https://doi.org/10.1016/j.energy.2022.125692>.
- [16] V. Reyes, J. J. Rodríguez, O. Carranza, and R. Ortega, "Review of mathematical models of both the power coefficient and the torque coefficient in wind turbines," in *2015 IEEE 24th International Symposium on Industrial Electronics (ISIE)*, Buzios, Brazil, Jun. 2015, pp. 1458–1463, <https://doi.org/10.1109/ISIE.2015.7281688>.
- [17] J. G. Gonzalez-Hernandez and R. Salas-Cabrera, "Representation and estimation of the power coefficient in wind energy conversion systems," *Revista Facultad de Ingeniera*, vol. 28, pp. 77–90, Mar. 2019, <https://doi.org/10.19053/01211129.v28.n50.2019.8816>.
- [18] A. B. Asghar and X. Liu, "Estimation of wind turbine power coefficient by adaptive neuro-fuzzy methodology," *Neurocomputing*, vol. 238, pp. 227–233, May 2017, <https://doi.org/10.1016/j.neucom.2017.01.058>.
- [19] M. Huleihil, G. Mazor, M. Huleihil, and G. Mazor, *Wind Turbine Power: The Betz Limit and Beyond*. London, UK: IntechOpen, 2012.
- [20] H. Bassi and Y. A. Mobarak, "State-Space Modeling and Performance Analysis of Variable-Speed Wind Turbine Based on a Model Predictive Control Approach," *Engineering, Technology & Applied Science Research*, vol. 7, no. 2, pp. 1436–1443, Apr. 2017, <https://doi.org/10.48084/etasr.1015>.
- [21] Z. Dekali, L. Baghli, and A. Boumediene, "Experimental Implementation of the Maximum Power Point Tracking Algorithm for a Connected Wind Turbine Emulator," *Revue Roumaine des Sciences Techniques, Série Électrotechnique et Énergétique*, vol. 66, no. 2, pp. 111–117, Jul. 2021.
- [22] P. K. Behera, B. Mendi, S. K. Sarangi, and M. Pattnaik, "Robust wind turbine emulator design using sliding mode controller," *Renewable Energy Focus*, vol. 36, pp. 79–88, Mar. 2021, <https://doi.org/10.1016/j.ref.2020.12.004>.
- [23] A. Mesbahi, M. Khafallah, A. Saad, and A. Nouaiti, "Emulator design for a small wind turbine driving a self excited induction generator," in *2017 International Conference on Electrical and Information Technologies (ICEIT)*, Rabat, Morocco, Aug. 2017, pp. 1–6, <https://doi.org/10.1109/EITech.2017.8255224>.
- [24] Z. B. Duranay, H. Guldemir, and S. Tuncer, "Implementation of a V/f Controlled Variable Speed Induction Motor Drive," *EMITTER International Journal of Engineering Technology*, vol. 8, no. 1, pp. 35–48, Jun. 2020, <https://doi.org/10.24003/emitter.v8i1.490>.